Improved d+^{4}He potentials by inversion, the tensor force and validity of the double folding model.

V.I.Kukulin, V.N.Pomerantsev
Institute of Nuclear Physics, Moscow State University, Moscow 119899, Russia.

S.G.Cooper
Physics department, The Open University, Milton Keynes MK7 6AA, UK.

S.B.Dubovichenko
Dept. of Physics, Kazakh State Iniv., Almaty.

(February 9, 2008)

Abstract

Improved potential solutions are presented for the inverse scattering problem for d+^{4}He data. The input for the inversions includes both the data of recent phase shift analyses and phase shifts from RGM coupled-channel calculations based on the NN Minnesota force. The combined calculations provide a more reliable estimate of the odd-even splitting of the potentials than previously found, suggesting a rather moderate role for this splitting in deuteron-nucleus scattering generally. The approximate parity-independence of the deuteron optical potentials is shown to arise from the nontrivial interference between antisymmetrization and channel coupling to the deuteron breakup channels. A further comparison of the empirical potentials established here and the double folding potential derived from the M3Y effective NN force (with the appropriate normalisation factor) reveals strong similarities. This result supports the application of the double folding model, combined with a small Majorana component, to the description even of such a loosely bound projectile as the deuteron. In turn, support is given for the application of iterative-perturbative inversion in combination with the double folding model to study fine details of the nucleus-nucleus potential. A d-^{4}He tensor potential is also derived to reproduce correctly the negative ^{6}Li quadrupole moment and the D-state asymptotic constant.

25.45.De,24.10.-i,21.60.Gx,24.75.+i

Contents of the paper.

1. Introduction
2. The role of parity dependence in IP inversion
3. Stabilised inversion of the d-^{4}He empirical data for $0 < E_d \leq 15$ MeV
4. Inversion of RGM $S(l)$ with breakup channel contributions
5. Validity of double folding model for d-^{4}He interaction and similar systems.
6. Tensor d-^{4}He potential and the ^6Li-quadrupole moment.
7. Conclusions

I. INTRODUCTION

Many basic features of the interactions between light composite particle are now well established. In particular, a good description [1]- [6], of the interactions of light nuclei such as $d + t$, t+^{3}He, ^{4}He+^{4}He etc. is obtained from a deep attractive potential with Pauli-forbidden states with the addition of parity dependence, Young scheme splitting and a spin-orbit interaction. Importantly, this type of interaction is now justified from microscopic considerations, both in quasi-classic picture [4] and also in quantum mechanical shell-model framework [1,7]. These results lead to a general comprehensive understanding of the relations between various interaction models which appear, at a first glance, to contradict to each other.

Nevertheless, a number of finer features of the interaction, notably the role of the dynamic polarisation of loosely bound projectiles such as d or ^{6,7}Li when combined with antisymmetrization effects, are not yet fully understood despite many previous efforts. The existing problems and contradictions are illustrated by the following example. On the one hand, it is well known (see e.g. [1], [8]- [13]) that antisymmetrization and coupled-channel effects in composite particle scattering unavoidably result in complex nonlocal and energy-dependent potentials, in which the breakup channels (with their various final angular momenta) lead to rather peculiar contributions in r-space and the specific energy dependence. On the other hand, for a long time it has been standard practice to describe the elastic scattering of deuterons and nuclei such as ^{6}Li by the standard optical model (via local potentials) with a smooth energy dependence, or even by global optical models [14].

The low energy N+^{4}He interaction presents a further example of these problems. An attempt undertaken long ago by Satchler *et al*, [15], to describe N+^{4}He phase shifts for E_N <20 MeV by a standard optical potential of Woods-Saxon form, required a significantly energy dependence in the *radial form* of the potential (i.e. of geometric parameters). Further studies based on S-matrix to potential inversion, [16,17], showed that the N+^{4}He phase shifts can be described excellently over a wide energy range (E_N <65 MeV) with a gaussian-like potential with odd-even splitting and with a small energy dependence in the potential depth alone. This odd-even splitting effect is a direct consequence of antisymmetrization, [1,5,18].

Thus the artificial energy dependence found by Satchler *et al* [15] reflects only the effect of omitting the odd-even splitting in the N+^{4}He potential.

Similar problems are also expected to arise for d+^{4}He and analogous systems. Moreover, many previous studies of deuteron scattering have demonstrated [12,13,19] the strong contribution of deuteron breakup channels, in particular with Δl=2, i.e. through the excitation of the D-state in N-N subsystem.

We can then ask, in what way can the above strong nonlocal contribution be incorporated into, say, the double folding potential, which, from a first glance, contains no such effects? (In this connection we must emphasise that the usual type of nonlocalities considered in literature [9,10] differs from the energy-singular terms arising when the virtual breakup channels are excluded). An important problem then arises to formulate the above nonlocal and specific energy dependent effects into a language of "exact" optical potentials. By this term we do not mean a standard phenomenological optical potential with a prescribed form (and fitted parameters) but instead some "exact" potential which is reconstructed by inversion from the data or from microscopic theory.

Our plan of study is as follows. As a first approach iterative perturbative (IP) inversions are presented, based on phase-shift analyses of experimental data. These inversions follow Ref. [16], in directly calculating an explicit Majorana exchange force, instead of applying separate inversions for even and odd partial amplitudes as in previous determinations of the empirical $d + \alpha$ potential, [20]. In this way the even and odd partial amplitudes are treated simultaneously and the inversion process is considerably stabilised. In the second approach, an extended RGM-study is presented for the same system in order to gain a deeper understanding of the complicated interplay between antisymmetrization and projectile breakup effects. Increasing the number of coupled channels in these RGM calculations leads to three sets of microscopic models for the $d-^4$He interaction:

- the direct $d-^4$He potential without incorporation of any exchange effects and which is related to standard double folding (DF) models (see e.g. [21]);

- the one channel (d+^{4}He) RGM model with full antisymmetrization but with a "frozen" deuteron and

- the multichannel RGM model inclusive of breakup channels.

RGM potentials are determined by inversion from the phase shifts of the last two models. The comparison of these different potential models then yields the contributions of antisymmetrization and deuteron breakup effects in terms of the local potential. Our approach has one further advantage, since the considerable flexibility of the inversion method allows the determination of potentials, which describe the system under study not at a single energy but for a wide energy range simultaneously (previously denoted as "mixed case" inversion [17,22,23]). The further comparison of our new parity dependent solutions obtained from the empirical data set and the RGM phase shifts allows *quantitative* deductions to be made on the validity of the DF model for the deuteron projectile (as applied in [24] for example).

The final part of our study is dedicated to a reconstruction of the tensor part of the d-^{4}He interaction. Here we study the range and depth of the d-^{4}He tensor force and compare it with the same quantities for central and spin-orbital components of the same system.

The contents of this work are then as follows. In Section II we describe, in brief, our inversion method and discuss the importance of including odd and even partial waves simultaneously in the inversion. Section III describes the empirical input data used and presents a new solution for the empirical case. Section IV is devoted to inversion of RGM calculations for d+^{4}He, which include coupling to the virtual breakup channels. Section V contains a detailed discussion of validity of the DF model. In Section VI, we describe the calculation of a tensor d-^{4}He potential which nicely fits the ^{6}Li quadrupole moment and the tensor mixing parameter ε_1. Our findings are summarised in a concluding section.

II. THE ROLE OF PARITY DEPENDENCE IN IP INVERSION

The inversion method used in the next sections has been developed in Moscow (in the Moscow State University) [20,22,23,25] and independently in the Open University by Mackintosh and coworkers, (originally in Ref. [26], with further developments and references in Ref. [16]). It has been named as the iterative-perturbative (IP) method by the latter group and as the linearised iterative method by the Moscow group. The two approaches have only minor differences which relate to the choice of inversion basis and details of the iteration process. The overall method is extremely flexible and convenient to use. It enables us to reconstruct many types of potentials, central, spin-orbit and tensor, real and complex, both from phase shifts or directly from scattering observables. The appropriate input quantities, e.g. S-matrix, differential cross sections, analysing powers etc. are nonlinear functions of the interaction potential and so may be considered as a functional response to variations in the interaction potential. In general, excluding some special cases, a small variation of the interaction potential is directly related to a small variation of the S-matrix or other response function.

The basic idea behind the approach is then a local linearization of the response function in neighbourhood of a given point in an appropriate functional space. This local linear approximation, together with an expansion of the unknown potential in some complete basis (for example the Fourier expansion in an orthogonal basis, [20,22,23,25] although gaussian functions worked well in inversions for p + α, [16]), results in a set of linear algebraic equations to be solved to give the expansion coefficients. The initial approximation (i.e. initial values of the expansion coefficients or a starting reference potential) is usually chosen based on physical considerations. In particular, as will be shown in later sections, the results of the present paper suggest that a good choice for the initial potential would be the DF potential. The initial potential is then corrected with step-by-step iterations. The iteration procedure converges rapidly (5 – 7 iterations at most are usually required) and gives a stable solution for the first expansion coefficients of the sought potential, where the number of reconstructed coefficients depends directly on the completeness and consistency of the input data.

The approach developed by the Moscow group has also been successfully applied, [27] to reconstruct interactions in the field of heavy ion scattering in systems such as ^{12}C+^{13}C, ^{16}O+^{17}O etc. The algorithm developed at the Open University has also been applied to a wide range of systems; for example to p + ^{16}O directly from experimental observables, [28], to mixed case N-nucleus phase shifts calculated from non-local interactions, [29], and to

single energy empirical S-matrices, for nuclei such as ^{16}O+^{16}O, [30], and for ^{11}Li scattering, [31].

A. The role of odd-even potential splitting.

The presence of well expressed low-energy resonances in the L=2 partial waves and near the S-matrix pole in the S-wave has been shown previously [20,23,25] to render the solution of the inverse problem for the above channels so reliable that the data for even a small energy interval 0-5 MeV is sufficient to give quite a correct reconstruction of d-^{4}He interaction potential in even partial waves. In sharp contrast to this, the odd partial amplitudes are derived from the phase shift analysis with large errors due to a low sensitivity of majority of observables (cross sections and tensor analysing powers) to these odd-parity partial phase shifts. As a result, the odd parity solution of the inversion has large errors which become more enhanced at the higher energies [20,25]. Hence, when the odd and even partial amplitudes are treated *independently* in the inversion [20,23,25], the magnitude and radial form of the Majorana interaction term cannot be established with sufficient accuracy. However, the structure of this term is very important for our understanding of the role and significance of exchange effects in nucleus-nucleus interactions.

The general form of operator (or potential) of particle interaction can be expressed as follows:

$$V = V_W + \hat{M} V_M \tag{1}$$

where V_W is the Wigner type interaction which includes the central, spin-orbit and tensor interaction terms, i.e.,

$$V_W = V_W^{(c)} + V_W^{(sl)} \mathbf{l}\cdot\mathbf{s} + V_W^{(t)} \hat{S}_{12}, \tag{2}$$

V_M is the Majorana type interaction which includes, in general, similar terms, i.e. central, spin-orbit and tensor, and $\hat{M}$ is the Majorana exchange operator. In the case here, for the interaction of two nuclei, a and b, $\hat{M} = P_{ab} = (-1)^{l_{ab}}$ and l_{ab} is a relative angular momentum of the pair a and b. Furthermore, in the standard approach the operator (1) can be rewritten in the form:

$$\begin{aligned} V &= \left(V_W^{(c)} + P_{ab} V_M^{(c)}\right) + \left(V_W^{(ls)} + P_{ab} V_M^{(ls)}\right) \mathbf{l}\cdot\mathbf{s} + \left(V_W^{(t)} + P_{ab} V_M^{(t)}\right) \hat{S}_{12} \\ &= \sum_{k=c,ls,t} \left(V_W^{(k)} \pm V_M^{(k)}\right) A^{(k)} \end{aligned} \tag{3}$$

where the operators

$$A^{(k)} = \begin{cases} 1, & k = c \\ \mathbf{l}\cdot\mathbf{s}, & k = ls \\ \hat{S}_{12}, & k = t^1 \end{cases} \tag{4}$$

and the plus sign relates to even partial waves and minus sign to odd partial waves. Now the interaction in the odd and even partial waves are uncoupled and each one can be parametrised and determined *independently* from the other[2].

The procedure by which two inversions are applied to establish the odd and even components of interaction potentials will be denoted here as "*separate*" inversion. This method has been previously applied to p+^{4}He [17] and d+^{4}He [20,25]. However, as discussed above, the separate determination of even and odd potential components induces significant errors in the appropriate potential if one set of partial amplitudes, viz. odd or even, with $J = L+1$ or $J = L-1$ etc. is determined from the phase shift analysis with considerable errors and this is quite often the situation.

The alternative approach is to derive the odd and even potential components simultaneously using the original form of interaction operator (3), i.e. to be denoted "*simultaneous*" inversion, and this procedure was first introduced in Ref. [16]. For the inversion of p+^{4}He empirical phase shifts the two approaches lead to very similar potentials. However simultaneous inversion was necessary to provide a stable parity-dependent inversion of p+^{16}O scattering observables, [28], because the Majorana term is very small in comparison to the Wigner type interaction. On the same note, it is common practice to apply inversion to all members of the families of partial amplitudes, $J = L+1$ and $J = L-1$ simultaneously, i.e. to determine central and spin-orbit potentials directly rather than to calculate potentials for the separate spin channels with $J = L-1$ or $J = L+1$ and so on.

The general philosophy behind the simultaneous inversion approach is the following. While the Majorana components describe exchange terms in the nucleus-nucleus interaction, [5,12], these components represent only a minor effect of the exchange correction compared to that contributing to the main Wigner term, which appears in the conventional simple and double folding models for nucleus-nucleus interactions. This difference suggests that a more stabilised inversion is obtained by expanding V_W and V_M in separate basis sets, as in Ref. [28], with different scale parameters in each case, i.e.

$$V_W(r) = \sum_{i=0}^{N_1} C_i^{(1)} \phi_i^{(1)}(r) \tag{5}$$

$$V_M(r) = \sum_{j=0}^{N_2} C_j^{(2)} \phi_j^{(2)}(r) \tag{6}$$

Here $\phi^{(1)}$ and $\phi_j^{(2)}$ are basis sets with appropriate radial scale parameters.

---

[1]In Sect. VI we use the standard S_{12} form for the tensor operator. A full classification for the tensor force based on symmetry principles was given by Satchler, [10]. See also Robson, [32]

[2]Formal mixing of odd and even partial waves is excluded due to parity conservation in nuclear interaction. Here we neglect a very small degree of mixing of the odd and even components due to the parity nonconserving terms.

This approach then leads to more reliable determination of the radial form and range of V_W and V_M compared to the potentials resulting from the separate inversion which may have significant uncertainties in the Majorana component. The inversion of empirical d+^{4}He phase shifts, described further in the following section, well illustrates the importance of simultaneous inversion. The improvement arises because both components are simultaneously determined from even (well determined) and odd (poorly determined) partial amplitudes on the equal footing. If one then combines such simultaneous determination with a step-by-step extension of the basis in (5) and (6), which is equivalent to the demand of maximal smoothness for each component, V_W and V_M, the inversion is stabilised.

III. STABILISED INVERSION OF THE D-^{4}HE EMPIRICAL DATA FOR $0 < E_D \leq$15 MEV

A. The empirical d+^{4}He phase shifts

In the next section we reconstruct the d-^{4}He interaction potential from phase-shift analysis (PSA) data using the algorithm developed by the Moscow group. The inversions are based on two separate sets of phase-shift data:

(i) single energy PSAs of the Zürich group [33] established for the energy range 6 - 43 MeV and

(ii) the extended energy-dependent PSA of Kuznetsova *et al* [34] for 0 - 10 MeV, with a special emphasis on the lowest energy region.

As in previous inversions based in this PSA, tensor potential terms are excluded from all the inversion calculations presented here except those described in Sect. VI, since the available data on the mixing parameters are too unreliable to produce a stable inversion. This problem arises due to the very weak influence of the tensor interaction on the low-energy phase-shifts, e.g. ε_1 differs from zero only in the narrow region near 6.5 MeV, where the $^3S_1$ and $^3D_1$ phase shifts are close in value. For similar reasons, only real potentials are determined due to the limitations in the inelasticity parameters. However, in Sect. VI we present a reconstruction of the ^{4}He + d tensor potential from the ^{6}Li quadrupole moment and the existing PSA data for the ε_1 mixing parameter.

Although the PSA-solutions of Zürich group contain many irregularities and some non-monotonic behaviour, especially for $E_d > 20$ MeV, the phase shifts in the energy range 6 - 14 MeV [33] are satisfactorily smooth functions of energy. On the other hand, the energy-dependent PSA [34] gives very reliable S- and D-wave phase shifts for $E_d < 6$ MeV, which strongly stabilises the inversion for both even and odd partial waves (see Sect. II). Therefore in this work we present results for inversions based on the phase shifts at energies up to 15 MeV only. A reconstruction of the d-^{4}He interaction using all the Zürich PSA data (up to 43 MeV), but by separate inversion, has been presented previously, [20].

B. Inversion from the d+^{4}He phase shift analysis data.

In this section we compare two solutions of the d+^{4}He inverse problem, for the energy range $0 < E_d \leq 15$ MeV, obtained as follows:

(i) by separate inversion of odd and even partial amplitudes, [20],

(ii) by simultaneous inversion of both amplitudes (present work).

As a starting approximation we take only one term in the expansions of each potential component, e.g. central, spin-orbit etc. Following our initial suggestions, [22] we have used a s-wave orthonormal harmonic oscillator basis, for which the first term of the series corresponds simply to a gaussian. Then, in each subsequent stage, we add one term to each of the above components (either to each component alternately or to all components at once). Such a procedure converges very rapidly and enables us to reliably control the process. If the input information is insufficient to determine the next expansion term, either the iterations fail to converge or the uncertainties in the expansion coefficients become too large, $\sim 100\%$, [22]. The convergence of the method had been investigated previously [22,23] and here we only give the final results of the inversion.

In Figs.1a, 1b and 2a, 2b we compare the potentials found for these two cases (the central components are displayed on Fig. 1 while the spin-orbit components are shown on Fig. 2).

The degree to which these two potentials reproduce the phase shifts is shown on Figs. 3 and 4 for the even and odd l-values respectively. The apparent disagreement between the predictions of the inversion and the data of the phase shift analyses for the P-waves, (Fig. 4), probably arises due to the large errors in the PSA data for these amplitudes, [33,34]. In particular, the results of accurate Faddeev calculations for d-^{4}He scattering [7,35] show a much better agreement with our predictions than with the PSA. So our simultaneous inversion for the P-waves may be closer to the "true" solution than is apparent from Fig. 4.

It is evident from Figs. 1 and 2 that the modifications to the potentials found when switching from the separate inversion to the simultaneous approach are rather small only for the even central potential, and are quite significant for the even spin-orbit and all the odd components. This improvement is due to the stabilisation of the simultaneous inversion.

Strong changes are also found in the odd potential on inclusion of the F phase shifts in the inversion (the dashed curve in Fig. 1b), when compared with inversion based on the P wave amplitudes alone (the dotted curve in Fig. 1b). These effects arise despite the large errors in the F-phase shifts of the PSA [33]. Clearly, the incorporation of such additional and *independent* input data for the inversion results in a further strong stabilisation of the inversion.

The above conclusion is in agreement with our initial general expectation that incorporation even of rather "noisy" but *independent* input data into the inversion, together with some definite additional constraint (e.g. requiring some degree of smoothness in the potentials), leads to a noticeable stabilisation of the solutions. This general feature of the IP inversion procedure then convincingly distinguishes our approach from more traditional and strict methods like Gel'fand-Levitan or Marchenko approaches. In the applications of the latter procedures, it is impossible to incorporate essentially incomplete or "noisy" data into the initial data set.

Turning now to the spin-orbit potential, we find a further illustration of the above conclusions. In fact, our results show that the Majorana component of spin-orbit interaction cannot be reliably derived from the existing PSA data. The reasons for this are partly due to the errors in the PSA data, but also due to the small size of the Majorana spin-orbit term.

This small Majorana spin-orbit term is justified by a comparison of the Wigner and Majorana components for central potential (see Fig. 5). Both the inversions based on RGM-calculations (see Fig. 7 in Section IV) and those based on the PSA data lead to central interactions for which the strength of Majorana component is smaller than the Wigner term by an order of magnitude. This result confirms the general expectations that the role of the Majorana term is then as a minor correction to the main Wigner term. Evidently, if a similar relation between Wigner and Majorana terms exists for the spin-orbit interaction, there is no chance of determining a Majorana (i.e. exchange) spin-orbit term from the existing PSA data.

Thus, summarising our findings in this Section, we conclude that the effects of the odd-even splitting for d+^{4}He are rather moderate. The significance of the effects are also illustrated by the values of the volume integrals,

$$J^{(k)} = -\frac{4\pi}{A_T A_P} \int V^{(k)}(r) r^2 dr \tag{7}$$

for the different components $V^{(k)}$ of the inverted potential, Eqs. 1-4. Table I displays the magnitudes of volume integrals J_k, for the potentials reported above and these values corroborate the above conclusions.

We have also estimated the value of $J^{(c)}$ for the Majorana terms of the potentials determined by simultaneous inversion. These potentials give,

$$J^{(c)}_{even} - J^{(c)}_{odd} = 2J^{(c)}_M \simeq 0.17 J^{(c)}_W,$$

i.e. J_M is about 8.5 % of J_W. Hence, as was expected beforehand, the Majorana term represents just a small correction to the main Wigner component.

The same interrelation between the Wigner and Majorana components should also be valid for the spin-orbit interaction and our stabilised inversion tends to corroborate this conclusion. While the difference in J for the spin-orbit terms obtained from separate inversion of even and odd partial waves is quite remarkable (see Fig. 2), this difference disappears for the potentials obtained by the simultaneous inversion. (Strictly speaking, it is beyond the accuracy achievable with the existing PSA – see the Table I.) Thus we may conclude that the initial assumption on which the simultaneous inversion of even and odd parity states was based, i.e. that the interaction is of mainly Wigner type, is well justified by the results of the inversion.

IV. INVERSION OF RGM $S(L)$ WITH BREAKUP CHANNEL CONTRIBUTIONS

The resonating group method (RGM) offers fundamental advantages for the study of the important effects contributing to d+^{4}He scattering, despite the simplified approximations

necessary in the method. Here contributions to the potential due to both the full antisymmetrization of all nucleons and the inclusion of breakup channels can be directly assessed in a way not possible by inversion from empirical phase shifts. This formulation of the d+^{4}He RGM calculations closely follows the work of Kanada *et al*, [36], and the breakup channels are included using the pseudo-state method described therein. Only $\Delta l = 0$ transfer is included in the breakup calculations.

The RGM S-matrices are numerically calculated using modified forms of the codes of Blüge *et al*, [37], adapted to incorporate the Minnesota NN force, [38] as described in a previous work, [39]. The exchange mixture parameter u is set to 0.97, but the potentials described below are not sensitive to this value. The deuteron and excited n-p pseudo-states are described by an 8 gaussian basis, [40], which allows coupling to 4 distortion channels of low energy deuteron excitation. No spin-orbit force is included in these calculations since the empirical spin-orbit terms cannot be determined to sufficient accuracy.

Tabulated S-matrix values are obtained from the RGM code for input into the IP inversion and, as in Sect. III, the inversion is confined to the energy range $0 < E_d < 15$ MeV. With inclusion of channel coupling the S-matrix becomes complex. At energies less than 10 MeV $|S|$ is close to unity, but at higher energies, the coupling to breakup channels produces an irregular variation of $|S|$ with energy. At the higher energies the imaginary potential arising from breakup coupling has been shown to have a marked variation with energy, [41]. The imaginary potential cannot then be established to any reliable accuracy over the energy range currently considered and all inversions in this section establish real potential components only.

The theoretical RGM phase shifts can be reproduced by inversion to a far greater accuracy than the empirical $S(l)$. However the most accurate inversions lead to irregularly shaped potentials due to an inherent, but small, energy dependence associated with the underlying nonlocality. The energy dependence of $S(l)$ cannot be reproduced by simply introducing an energy dependence in the potential magnitude, but requires a variation in the *potential form* with energy. Since the details of such a dependence are far beyond what can be determined empirically, only smooth energy independent solutions are now considered and these lead to an adequate fit to the phase shifts.

Solutions are obtained for both the two inversion methods described in Sect. II i.e. for separate inversion of even and odd l-values and for simultaneous inversion to determine V_W and V_M. The choice of method is less critical in the case of theoretical $S(l)$ and, with a small inversion basis, (2 functions per component) the two methods lead to very similar parity dependent potentials. The simultaneous inversions also show that a reasonable fit to the RGM $S(l)$ is possible with a V_W term alone, so that the addition of the V_M component introduces only a second order correction.

Fig 6 shows the even and odd l potentials for all four cases, with and without breakup coupling and using the two inversion approaches. The components V_W and V_M for the potentials obtained by simultaneous inversion are illustrated in Fig. 7 together with the RGM direct potential obtained from the double folding model for the Minnesota NN force. The breakup channels primarily change the even l phase shifts only, [36], so that, although the even potential *increases* significantly in magnitude on inclusion of breakup coupling, there is little change in the odd component.

The restriction to energy-independent potentials leads to some uncertainties in the inver-

sion but some interesting results are revealed. The introduction of coupling produces both an increase in the Wigner potential magnitude at small radii and a small decrease at $r \sim 3$ fm. However, at larger radii the solution inclusive of breakup coupling is very close to the direct potential multiplied by $N_{\rm DF}$=1.572 (see also Fig. 1).

The large changes in the even l phase shifts due to breakup coupling significantly decrease the parity dependence (i.e. the amplitude of the Majorana force) for $r < 2$ fm. At larger radii there is a considerable agreement in the parity dependence for all solutions, but the strength of the V_M term barely exceeds 1 MeV.

We can now compare the RGM potentials with the empirical solution presented in Sect. III, which is indicated as the dotted line in Fig. 7. The limitations of the RGM calculations and its dependence on simple interactions, preclude the possibility of a very exact agreement with empirical results. Indeed the magnitude of V_M is too small at both larger radii and near the nuclear centre, although the latter problem is improved by the addition of breakup coupling. Significantly, the inclusion of breakup effects brings the Majorana component closer to the empirical V_M potential, although the RGM potential is still too small in magnitude for $r < 2$ fm. As a consequence, the net effective d-^{4}He RGM potential is close to a conventional *local* parity-independent potential.

A poorer agreement is found between the RGM solutions and the empirical potential resulting from separate inversion, particularly for the Majorana component, which presents further evidence in favour of the simultaneous inversion.

V. VALIDITY OF DOUBLE FOLDING MODEL FOR D-^{4}HE AND SIMILAR SYSTEMS.

In the last two or three decades the DF-model has become extremely popular for the description of optical scattering, not only for p, ^{3}He(^{3}H), ^{4}He etc., but also for such loosely bound particles as d, ^{6,7}Li or ^{9}Be [1,10,11], [42]- [46]. However, for the latter projectiles the normalisation constant $N_{\rm DF}$ was found to deviate considerably from unity and is anomalously low. This problem has been explained [9,19,26,42,43], by the strong coupling effects of the virtual or real breakup of the loose projectile.

The accurate and fairly reliable potential for d-^{4}He established by inversion now allows us to study the behaviour of the normalisation constant in a more quantitative manner than was possible in the simple phenomenological analyses of deuteron scattering by medium and heavy nuclei [14].

The most important question here is how adequate is the DF potential form? The general success of the DF model apparently argues in favour of its correctness. Nevertheless the situation here is far from trivial. In fact, the DF potential (which corresponds to the so called no-distortion approximation) must adequately describe only the peripheral part of inter-nuclear interaction where there is no distortion of the colliding nuclei. Moreover, to achieve this it is necessary to use an NN-potential which has the correct peripheral behaviour, and the normalisation factor $N_{\rm DF}$ should be close to unity. Then one hopes that the short range part of the inter-nuclear interaction, where the effects of distortions and breakup are of greater importance, will be screened by a strong imaginary potential. In such circumstances the DF model will be a good approximation for the exact interaction.

However, most practical applications of the DF procedure are based on an effective *scalar* NN-potential (usually the M3Y-force) which is quite dissimilar to the true NN-force. The DF potential calculated in this way must then be renormalised with some constant $N_{\rm DF} \neq 1$.

In such an approach the degree of similarity between the "exact" potential and the DF potentials in both the peripheral and short-range radial regions is very interesting. Below we will try to answer these important questions.

In the Fig. 1a a DF potential, calculated with the effective NN Minnesota force, is compared with the stabilised solution of the inverse scattering problem described in Sect. II. It is evident that the *initial* DF potential, even in the far peripheral region, is very different from the "true" interaction potential and the difference is rather large in the inner region. Now, following to the standard routine [14], we can also calculate the normalisation coefficient $N_{\rm DF}$ for which this DF potential best reproduces the phase shifts data. The even-parity partial amplitudes are most accurately reproduced with $N_{\rm DF}$=1.572.

The quality of fit to the phase shifts reached with this value of N_{DF} is displayed in Fig. 8. Clearly, with the exception of the S-waves, the renormalised DF-potential provides a very reasonable fit to these phase shifts. In fact, the direct comparison of the renormalised DF-potential with potential obtained by inversion (see Fig. 1a) reveals that the peripheral parts ($r \geq 3$ fm) of both potentials are in reasonable agreement. In the inner region, however, there are large differences between the potentials and these differences are reflected in the S-wave phase shift behaviour. The D wave and all higher partial phase shifts are not influenced by these short range differences. The role of the short range region will be further reduced by the imaginary potential which is present for $E_d > 3.5$ MeV and which will screen out the short range part of the potential.

Thus, the rather good agreement of both DF and inversion potentials at intermediate and large distances, and in the phase shift behaviour, does support the application of the DF procedure for the description of deuteron scattering, even by the very light ^{4}He-nucleus.

Further evidence is provided by a comparison of volume integrals, J, for the various potentials, as shown in Table I. In fact, the volume integral of the even parity potential, as determined by simultaneous inversion, is very close (with a difference of $\sim 1\%$ only) to that of the DF potential [24], calculated with the standard (density-dependent) DDM3Y NN effective force and with $N_{\rm DF}$ adjusted to reproduce the even l phase shifts. The equivalent comparison for the odd parity phase shift shows far less agreement, and the volume integral of that M3Y DF potential for odd l is closer to the volume integrals for the even parity cases. The volume integrals for the DF potentials calculated with both the Minnesota and M3Y-potentials and (after multiplication by appropriate normalising factors $N_{\rm DF}$) are close to each other. However the DF model with the M3Y force is expected to give a better agreement with the data than the Minnesota force.

We can now turn to the role of deuteron breakup channels and antisymmetrization effects. The basic problem here, as was emphasised earlier, is how to reconcile the apparent contradiction between the rather good fit to scattering data given by the double folding model (with the M3Y force), on the one hand, although highly renormalised, [10]- [11], [43], [44]- [46] and the proven contributions of the large effects of the virtual deuteron breakup channels, [11]- [13]. In fitting the phase shifts with the DF model only the NN effective force constant is adjusted, so that a good description of data means that the *radial form* of

deuteron polarisation potential[3] must be similar to the potential giving rise to purely elastic scattering, i.e. without any channel coupling. Thus the renormalised force constant in DF potential should effectively incorporate three important effects:

(i) coupling with virtual breakup channels;

(ii) antisymmetrization effects;

and closely connected with the latter,

(iii) the odd-even splitting effect.

Our conclusions derived here together with the results of other authors can be summarised as follows:

- the Majorana force component, although definitely contributing, plays a rather moderate ($\sim 8\%$) role and hence does not destroy the good quality of fit achieved with the pure central interaction potential of the DF approach;

- antisymmetrization and channel coupling effects as discussed in Sect. IV of the present work and also in Refs. [12,13] are rather large when considered separately, but the effects compensate each other to a considerable degree[4]. Thus, the resulting net effect is rather small (see Figs. 6 and 7).

The odd parity potential shows almost no change when the deuteron breakup channels are included, whereas the even potential changes, on average, by 15-25% at small radii. The reason underlying this change is seen in Fig. 7 where one can see that both the Wigner term V_W and the Majorana term V_M deepen by $\sim$10 MeV near the origin on inclusion of channel coupling. However, the interaction in the even partial waves is described by the combination $V_W(r) + V_M(r)$ while that for the odd partial waves is governed by the combination $V_W(r) - V_M(r)$. As a result, the channel coupling (CC) leads to a deepening of the even potential by $\sim$20 MeV near origin and to almost no change in the odd potential component. Thus, on average, the net effect of channel coupling is about 10%.

Moreover, as we have already observed, the net effect of CC is mostly short ranged (see the upper part of Fig. 6). Because this short range contribution is often screened by an imaginary potential and is effectively invisible, the long range contributions of CC can be simulated by renormalising the total NN force constant to reproduce the $d + A$ scattering cross sections. In fact, the one-channel effective d-^{4}He RGM potential (see the curves 1 and

---

[3]We assume quite naturally that the excitation of tightly bound nucleus ^{4}He at $E_d \leq$15 MeV can be safely ignored.

[4]This is quite clear from a physical point of view since inclusion of the deuteron breakup components with a large radial range leads to an effective stretching of the deuteron while the antisymmetrization with the compact α-cluster wavefunction acts in the opposite direction, i.e. produces a "compressing" effect on the deuteron .

2 on the upper part of Fig. 6), which takes into account only the antisymmetrization effects but not the coupling to breakup channels, is very similar to the renormalised DF potential (see the dot-dashed curve on Fig. 1a).

While the DF potential, as initially calculated, is somewhat different in form from the "true" interaction, especially in the inner region, by renormalising NN constant this difference can be minimised. In other words, the renormalised DF potential reproduces the"true" potential in the peripheral region (r >2.5 fm) quite well. However, the renormalised DF potential is a little deeper than the "true" one in the intermediate region 1.5 fm < r <2.5 fm and also more shallow by $\sim 20\%$ than the true potential in the innermost region, r <1.5 fm. Consequently, when the DF model is applied to deuteron scattering off light nuclei we expect to obtain quite a reasonable description of the elastic scattering cross section, but with some deviations from the data for the vector and especially the tensor analysing powers, which are sensitive to variations of the odd l phase shifts and to interference effects.

A careful comparison of the potentials determined from RGM phase shifts calculated *without* channel coupling effects (solid lines in the upper part of Fig. 6) with the renormalised DF-potential $V_{DF}(r)$ (the dot-dashed line on Fig. 1a) shows that the deviation of the DF potential from the true one is most likely to arise due to deuteron breakup channel coupling[5]. Therefore one expects the DF model to give a highly accurate description when applied to the description of scattering of more dense and heavily polarised projectiles such as α particles. Recent work, [45], confirms this conclusion.

Our main result in this section for the scattering of a loosely bound deuteron from the ^{4}He core can be formulated as follows: If the scattering is described by only a full antisymmetrization of the d+^{4}He clusters without breakup contributions, then the local equivalent potential must contain a large Majorana component and this scattering *cannot* be described by a simple parity independent optical potential. However, the addition of antisymmetrized breakup channels to the no-distortion approximation results in a strong reduction of the odd-even potential splitting and the resulting unified potential can be approximated reasonably well by a renormalised DF potential. In other words, only when both the antisymmetrization and d breakup contributions are considered together, can use of the DF model be justified.

VI. TENSOR D-^{4}HE POTENTIAL AND THE ^{6}LI QUADRUPOLE MOMENT

The d+^{4}He tensor interaction has been neglected in the preceding sections due to the lack of reliable mixing parameters in the present PSA data . On the other hand, a tensor potential is absolutely necessary to describe the quadrupole moment of ^{6}Li nucleus.

It is well known that the very small negative value of ^{6}Li quadrupole moment ($Q = -0.0644$ fm^2) cannot be explained by the standard three-body α + 2N model, [47], but probably originates through the coupling between the D-wave component of the α-particle in the closed channel $d + d \rightarrow ^4$He and the D-wave component of the $\alpha + d$ relative motion.

[5]This conclusion is in agreement with the results of analysis of the scattering of other weakly bound projectiles like ^{6,7}Li, ^{9}Be etc. [43,49].

The negative value of Q is associated directly with the negative value of the asymptotic mixing constant $\eta_D = -0.0125$ [48], i.e. the sign of the D-component of the bound-state wave function (in the asymptotic region) must be *opposite* to that of the S-component. A ^{6}Li wave function of this type has been formulated, [49] and this model does give the correct sign of quadrupole moment.

Here we attempt to reconstruct a d–^{4}He potential which describes the $^3S_1$ and $^3D_1$ low-energy phase shifts and the main properties of the ^{6}Li ground state, including the quadrupole moment. Consequently the data input into the inversion includes the binding energy and quadrupole moment of ^{6}Li together with the phase shifts for energies up to 11 MeV. To retain stability in the inversion, we have restricted the expansions of both central and tensor parts of interactions to just one term:

$$V(r) = V_c(r) + V_t(r)S_{12}, \tag{8}$$

$$V_c(r) = -V_0 \exp(-\alpha r^2) \tag{9}$$

$$V_t(r) = -V_1 \exp(-\beta r^2) \tag{10}$$

Table II lists the parameters of two possible potentials satisfying the above criteria. The properties of the ^{6}Li ground state calculated from these potentials are presented in Table III, together with the corresponding experimental values. The $^3S_1$ and $^3D_1$ phase shifts and the mixing parameter ε_1, evaluated with the two potentials, are shown in Figs. 9 and 10 (solid lines are for variant A, dashed line for variant B). The negative values of ε_1 can be obtained only from narrow tensor potentials. The use of wider potentials results in both a change of sign of ε_1 and a change of the asymptotic mixing constant of the ground state η_D. Thus the range of the d-^{4}He tensor potential is much less than that of the central potential. This finding provides evidence for a strong d-exchange contribution to the tensor d-^{4}He force [47][6] because the range of the exchange force in the exchange mechanism should be rather short due to the small r.m.s. radius of ^{4}He and the large binding energy in the channel ^{4}He$\rightarrow d+d$.

VII. CONCLUSIONS.

In this work we have studied some important problems relating to the interaction potential underlying the scattering of composite particles such as d+^{4}He. In order to establish the true interaction potential, we solved an inverse scattering problem using our effective method of linearised iterations. The input for the inversions include both phase shifts calculated from RGM coupled channel calculations, which incorporate virtual and real breakup channels, and the results of a recent phase shift analysis.

The success of the inversions presented here depended considerably on combining the very reliable even partial wave amplitudes with the "noisy" odd l values within the empirical data

[6] This effect should be compared with the NN one-pion-exchange forces where both central and tensor components have the same range, μ^{-1} (μ is the pion mass).

set. The Majorana exchange interaction was *explicitly* evaluated in the inversion, and by this procedure the odd parity potential is determined with greater stability. The resulting empirical potentials then represent an improvement on previous d+^{4}He potentials for which the odd parity potential was unreliable and inaccurate.

The new stabilised empirical potential can be applied to predict improved phase shifts for the odd partial waves. In fact, these predictions agree quite well with the RGM predictions, but only after inclusion of the breakup channel coupling, both in the Wigner and the Majorana components of the potential.

In fact, both the solutions (i.e. obtained from the RGM phase shifts and from the PSA data set) contain only a small magnitude for the Majorana component. Significantly, the breakup effects only contribute noticeably to the even parity potential and have little effect on the odd parity component. This odd-even splitting is then expected to be of minor importance for other $d + A$ systems.

We have also compared these "exact" interaction potentials with the potentials calculated using the popular DF model based on two different effective NN forces:

- DDM3Y NN-force, and

- Minnesota NN-force.

This comparison shows that, despite the models producing apparently different d-^{4}He DF potentials, on the whole the general agreement is reasonable. However, the DDM3Y force, multiplied by an appropriate normalisation factor, leads to a better agreement with empirical potentials and provide a quite satisfactory reproduction of the "experimental" phase shifts (see also [14,24], [44]- [46]). Nevertheless more detailed effects such as the odd-even splitting etc. are not included in the DF approach.

This agreement of the DF M3Y model with the empirical potential arises as a result of the interference of several effects, none of which is apparently taken into account in the DF model, notably antisymmetrization and breakup channels coupling. These two contributions mutually compensate each other in the relevant region of configuration space to the extent that the DF approach plus an appropriate normalisation factor provides a reasonable approximation to the required interaction potential.

An analysis of d+^{40}Ca scattering at $E_d = 52$ MeV, [44], lead to similar results to those presented here. In particular the interrelation between the DF potential for d+^{40}Ca and the "exact optical potential" extracted from the data by a model independent analysis equates strongly to our findings for $d + \alpha$. This comparison then suggests that our results may have a much wider applicability than the particular case considered here.

Combining the above results leads to a very powerful inversion procedure. The modified IP inversion method, as employed widely in the present work, converges very fast and in a stable manner with a good choice of initial potential. The DF model is now confirmed as a very convenient candidate for this initial approximation. The complete method, when invoked for inversion directly from cross-section data, [25,28], offers many opportunities to study fine details of the interactions of complicated systems such as ^{24}Mg+^{112}Sn, ^{12}B+A etc. and even for unstable radioactive projectiles scattered off stable targets (see e.g. [50]).

In this paper we have also determined a d-^{4}He tensor interaction. The resulting potential is rather short ranged and is relatively large in amplitude ($\sim 30 - 40$ MeV). As has been

previously suggested, [47], this interaction may arise due to the very specific exchange effect in which the "inner" deuteron in the D state of the ^{4}He core is exchanged with the outer valence deuteron. This exchange mechanism can be applied to explain both the short range character of the d-^{4}He tensor force, through the very small r.m.s. radius of ^{4}He, and the *negative* value of the ^{6}Li quadrupole moment. The second result is consistent with the fact that the s-wave and d-wave components of the total ^{6}Li wavefunction, when projected onto the d-^{4}He channel, have opposite signs in the asymptotic region. Thus the form and strength of the d-^{4}He tensor force at both low and intermediate energies deserve detailed study. The results presented here may be considered an initial step in this interesting direction.

Many characteristic features of interaction of the d-^{4}He system have been established in this and a series of preceding works [1,7,20,23,25,34,47]. In these works important features such as the Pauli principle manifestation and the appearance of Pauli-forbidden states, the description of higher partial waves, channel coupling effects, the interrelation with supersymmetrical partner potentials and the general manifestation of dualism repulsion-attraction in composite particle interaction have been studied in detail. In particular we have shown, [1,3], that the deep attractive interaction potentials in the systems ^{4}He+^{4}He, ^{4}He+N etc. arise as a consequence of well localised Pauli forbidden states and the appropriate conditions of orthogonality for the scattering wavefunctions to these forbidden states. In turn, the structure of the Pauli forbidden states is very closely interrelated to the shell model structure of the whole unified system [4,7]. Other interesting effects have been found involving the joint action of antisymmetrization and (virtual) breakup in ^{6}Li, [12]. For this case calculations have established that, while the inclusion of deuteron breakup channels *diminishes* the d+^{4}He cluster probability in the full three body ^{6}Li wavefunction, the subsequent antisymmetrization of the $n+p$+^{4}He wavefunction *increases* the d+^{4}He cluster probability. Again both these important contributions produce opposing effects. Thus the present paper can be considered, in some sense, as a concluding work in the long series of our studies for d+^{4}He and similar cluster systems.

ACKNOWLEDGEMENTS

The authors are grateful to Prof. V.Neudatchin, Dr. R.S. Mackintosh and our colleagues at the Moscow Institute of Nuclear Research for useful discussions in the course of the work.

REFERENCES

[1] V.I. Kukulin, V.G. Neudatchin, Yu.F. Smirnov, I.T. Obukhovsky *Clusters as Subsystems in Light Nuclei*. Vol. 3, In the series *Clustering Phenomena in Nuclei*, (Vieweg & S. Verlag, Braunschweig/Wiesbaden, 1983).

[2] B.Buck, C.B.Dover and J.P.Vary, Phys.Rev. C**11**, 1803 (1975); B.Buck and A.A.Pilt, Nucl.Phys. **A280**, 133 (1977).

[3] V.I. Kukulin, V.G. Neudatchin, A.A. Sakharuk and V.N. Pomerantsev, Phys.Rev.C**45**, 1512 (1992); Yad.Fiz. (Sov. J.Nucl.Phys.) **52**, 402 (1990); Phys.Lett.**B255**,482 (1991).

[4] H. Horiuchi, Progr.Theor.Phys. **64**, 184 (1980).

[5] Y.C. Tang, M. LeMere and D.R. Thomson, Phys. Rep. **47**, 167 (1978).

[6] S.G.Cooper, Phys. Rev. C**50**, 359 (1994).

[7] L.D. Blokhintsev, V.I. Kukulin, D.A. Savin and A.A. Sakharuk Yad.Fiz. (Sov. J. Nucl.Phys.) **53**, 693 (1991).

[8] H. Feshbach, Ann. Phys. **5**, 357, (1958).

[9] S.A. Sofianos, K.C. Panada and P.E. Hodgson, J.Phys.G: Nucl. Part. Phys. **19**, 1929 (1993).

[10] G.R. Satchler, *Direct Nuclear Reactions* (Clarendon Press, Oxford, 1983).

[11] T.K. Roy and S. Mukherjee, J.Phys.G.: Nucl.Phys. **13**, 1239 (1987); G.H. Rawitscher, Phys.Rev. C**9**, 2210 (1974); Nucl.Phys. **A241**, 365 (1975)

[12] R.G.Lovas, A.T. Kruppa, R. Beck and F. Dickman, Nucl.Phys. **A474**, 451 (1987); K Varga and R.G.Lovas, Phys. Rev. C**43**, 1201 (1991); Y. Fujiwara and Y.C. Tang, Phys. Rev. C**43**, 96 (1991); Few Body Systems, **12**, 21 (1992): H.Kanada, T.Kaneko and Y.C.Tang, Phys. Rev. C**38**, 2013 (1988).

[13] Y. Yahiro and M. Kamimura, Progr.Theor.Phys. **65**, 2046; 2051 (1981); V.I. Kukulin and V.N. Pomerantsev, Yad.Fiz. (Sov.J. Nucl.Phys.) **50**, 27 (1989).

[14] J.Cook, Nucl.Phys. **A382**, 61 (1982).

[15] G.R.Satchler, L,W. Owen, A.J. Elwyn, G.L. Morgan, and R.L. Walter, Nucl.Phys. **A112**, 1 (1968).

[16] S.G.Cooper and R.S.Mackintosh, Phys. Rev. C**54**, 3133 (1996).

[17] S.G. Cooper and R.S. Mackintosh, Phys. Rev. C**43**, 1001 (1991).

[18] S.G. Cooper, R.S. Mackintosh, A. Csótó, and R.G. Lovas, Phys. Rev.C **50**, 1308 (1994).

[19] A.A.Ioannides and R.S.Mackintosh, Phys. Lett. **169B**, 113 (1986).

[20] V.I. Kukulin and V.N. Pomerantsev, Yad.Fiz. (Rus.J. Physics of Atomic Nuclei) **60**, 1228 (1997).

[21] G.R.Satchler and W.G. Love, Phys. Rep. **55**, 183 (1979).

[22] V.I. Kukulin, V.N. Pomerantsev and J. Horaček, Phys.Rev. A**42**, 2719 (1990).

[23] V.I. Kukulin and V.N. Pomerantsev, Yad.Fiz. (Sov.J. Nucl.Phys.) **51**, 376 (1990).

[24] P. Mohr, V. Kölle, S. Wilmes, U. Atzrott, G. Staudt, J.W. Hammer, H. Krauss and H. Oberhummer, Phys.Rev. C**50**, 1543 (1994); Z.Phys. **A349**, 339 (1994).

[25] V.I. Kukulin, V.N. Pomerantsev and S.B. Zuev, Yad.Fiz. (Rus. J.Physics of Atomic Nuclei) **59**, 428 (1996).

[26] R.S.Mackintosh and A.M.Kobos, Phys. Lett. **116B**, 95 (1982).

[27] A. Adahchour, D. Baye and P. Descouvemont, Nucl.Phys. **A579**, 305 (1994).

[28] S.G. Cooper, Nucl. Phys. **A618** 87 (1997).

[29] R.S. Mackintosh and S.G. Cooper, J. Phys. G: Nucl. Part. Phys. **23**, 565 (1997).
[30] S.G. Cooper and R.S. Mackintosh, Nucl. Phys. **A576**, 308 (1994).
[31] S.G. Cooper and R.S. Mackintosh, Nucl. Phys. **A582**, 283 (1995)
[32] B.A. Robson, *The theory of Polarisation Phenomena*, (Clarendon Press, Oxford, 1974).
[33] B. Jenny, W. Grüebler,V. König, P.A. Schmelzbach and C. Schweizer, Nucl.Phys. **A397**, 61 (1983).
[34] E.V. Kuznetsova and V.I. Kukulin Yad.Fiz. (Rus. J.Physics of Atomic Nuclei), **60**, 528 (1997); V.M. Krasnopol'sky, V.I. Kukulin, E.V. Kuznetsova, J. Horaček and N.M. Queen, Phys.Rev. C**43**, 822 (1991).
[35] Y.Koike, Progr. Theor.Phys. **59**, 87 (1978).
[36] H. Kanada, T. Kaneko, S. Saito and Y.C. Tang, Nucl. Phys. **A444**, 209 (1985).
[37] G. Blüge, K. Langanke and H.-G. Reusch, "Computational Nuclear Physics 2", Ed. K. Langanke, J.A. Maruhn and S.E. Koonin (Springer-Verlag, New York) (1993).
[38] D. R. Thompson, M. LeMere and Y.C. Tang, Nucl. Phys. **A286**, 53 (1977).
[39] S.G. Cooper, OU preprint OUPD9707, Nucl. Phys. **A** (to be published).
[40] V.I.Kukulin and G.G. Ryzhikh, Prog. Part. Nucl. Phys. **34**, (1995) 397; V.I.Kukulin and V.N. Pomerantsev, Sov. J. Nucl. Phys. **50**, (1989) 17.
[41] R.S. Mackintosh and S.G. Cooper, OU preprint OUPD9708, Nucl. Phys. **A** (to be published).
[42] M. Kamal, V.T. Voronchev and V.I. Kukulin, VANT (Problems of At. Science and Technique), Ser. fusion. **No 3**, 37 (1989); J.Phys.G: Nucl.Part.Phys. **18**, 379 (1992).
[43] C. Samanta, S. Ghosh, M. Lahiri, S. Ray and S.R. Banerjee, Phys.Rev. C**45**, 1757 (1992); T.Sinha, S. Ray and C. Samanta, Phys.Rev. C**48**, 785 (1993).
[44] M.Ermer, H.Clement, P.Grabmayr, G.J.Wagner, L.Friedrich and E.Huttel, Phys.Lett. **B188**, 17 (1987).
[45] U.Atzrott, P. Mohr, H. Abele, C. Hillenmayer and G. Staudt, Phys.Rev. C**53**, 1336 (1996).
[46] H.Abele and G. Staudt, Phys.Rev. C**42**, 742 (1993).
[47] V.I. Kukulin, V.N. Pomerantsev, Kh.D. Razikov V.T. Voronchev and G.G. Ryzhikh, Nucl.Phys. **A586**, 151 (1995).
[48] H.R.Weller and D.R.Lehman, Ann. Rev. Nucl. Part. Sci. **38**, 563 (1988); R.Crespo, A.M.Eiro and F.D.Santos, Phys.Rev. C**39**, 305 (1989).
[49] N.Nishioka, J.A.Tostevin, R.C.Johnson and K.I.Kubo, Nucl.Phys. **A415**, 230 (1994).
[50] S.A. Goncharov, A.S. Dem'yanova and A.A. Ogloblin, " Nucleon density distributions in ^{8}He and ^{8}B from elastic scattering by ^{3}He and ^{3}H", Preprint INP MSU 97-31/4482, 1997, Moscow, Inst. Nucl. Phys. Moscow State Univ.

FIGURES

FIG. 1. (a) The central part of d-^{4}He potential for even partial waves reconstructed with PSA input data up to 15 MeV. The solid line is the result of simultaneous inversion (present work) and the dashed line represents the result of separate inversion, [20]. Also shown is the potential obtained by separate inversion including energies up to 33 MeV, [20] (dotted line), the DF potential with the Minnesota NN force (triple dot-dashed line) and this DF potential multiplied by $N_{\rm DF} = 1.572$ (dot-dashed line).
(b) The central part of d-^{4}He potential for odd partial waves reconstructed with PSA input data up to 15 MeV. Solid line is the results of simultaneous inversion (present work), dashed line is from a separate inversion of odd-parity P and F waves [20] and the dotted line shows the inversion based on the P- wave phase shifts only.

FIG. 2. (a) The d-^{4}He spin-orbit potential for even partial waves reconstructed with PSA input data up to 15 MeV. The notation is as in Fig. 1a.
(b) The d-^{4}He spin-orbit potential for odd partial waves reconstructed with PSA input data up to 15 MeV. The notation is as in Fig. 1b.

FIG. 3. The S- and D-wave phase shifts for the potential reconstructed by simultaneous inversion for energies up to 15 MeV (solid lines). Dashed lines show the results for inversion of even waves only [20]. PSA data are designated: • – from [34], △, ▲, ■, ♦ from [33] for S- and D_J-waves ($J = L-1, L, L+1$) respectively.

FIG. 4. Similar to the Fig. 3 but for the P-wave phase shifts.

FIG. 5. Wigner V_W (solid line) and Majorana V_M (dashed line) parts of central potential reconstructed from PSA input data up to 15 MeV.

FIG. 6. Even (upper panel) and odd (lower panel) parity potentials determined from single channel RGM $S(l)$, by the two inversion approaches, separate (solid line) and simultaneous (dashed line), and from RGM $S(l)$ with breakup channel coupling by separate(dotted line) and simultaneous inversion (dot-dashed line).

FIG. 7. The components V_W (upper panel) and V_M (lower panel) for simultaneous inversion from single channel RGM $S(l)$, (solid line) and from RGM $S(l)$ with breakup channel coupling (dashed line) compared with the empirical potential from simultaneous inversion (dotted line) and the RGM direct potential (dot-dashed line).

FIG. 8. Comparison between the S-, D- and G-wave phase shifts for the double folding potential multiplied by $N_{\rm DF} = 1.572$ (solid lines) and the "average" phase shifts calculated with central part of the reconstructed potential (dashed lines). (G-wave phase shifts are multiplied by 10 for convenience.)

FIG. 9. The theoretical eigen phase shifts δ_α and δ_β (corresponding to the $^3S_1$ and $^3D_1$ phase shifts in the uncoupled channels) and the PSA-results. The solid and open triangles display the PSA δ_α and δ_β respectively. The solid and dashed lines correspond to the tensor potentials A and B respectively.

FIG. 10. The comparison between the theoretical and experimental values of the tensor mixing parameter ε_1. The solid and dashed lines correspond to the tensor potentials A and B respectively.

TABLES

TABLE I. Values of volume integrals $-(4\pi/8)\int V(r)r^2dr$ [Mev·fm^3] for different d+^{4}He potentials

	simultaneous inversion, present work	separate inversion [20]	DF with Minnesota-force	DF with DDM3Y [24]
even waves	665.6	672.3	646.9	675.0
odd waves	546.3	573.3		614.0
spin-orbit	13.8	19.8		

TABLE II. Parameters of the tensor potential for d+^{4}He.

variant	V_0 [MeV]	α, [fm^{-2}]	V_1 [MeV]	β, [fm^{-2}]
A	-71.979	0.20	27.0	1.12
B	-77.106	0.22	40.0	1.60

TABLE III. The properties of the ^{6}Li ground state, calculated with the reconstructed tensor d+^{4}He potential

Properties	Potential A	Potential B	Experimental values
E_b, [MeV]	-1.4735	1.4735	1.4735
R_r, [fm]	2.60	2.56	2.56(5)
R_f, [fm]	2.53	2.50	2.54(5)
Q, [fm^2]	-0.064	-0.064	-0.0644(5)
C_0^0	1.9	1.9	2.15(10)
η_D	-0.0115	-0.0120	-0.0125(25)
μ_d/μ_0	0.848	0.847	0.822
P_D, %	1.59	1.78	

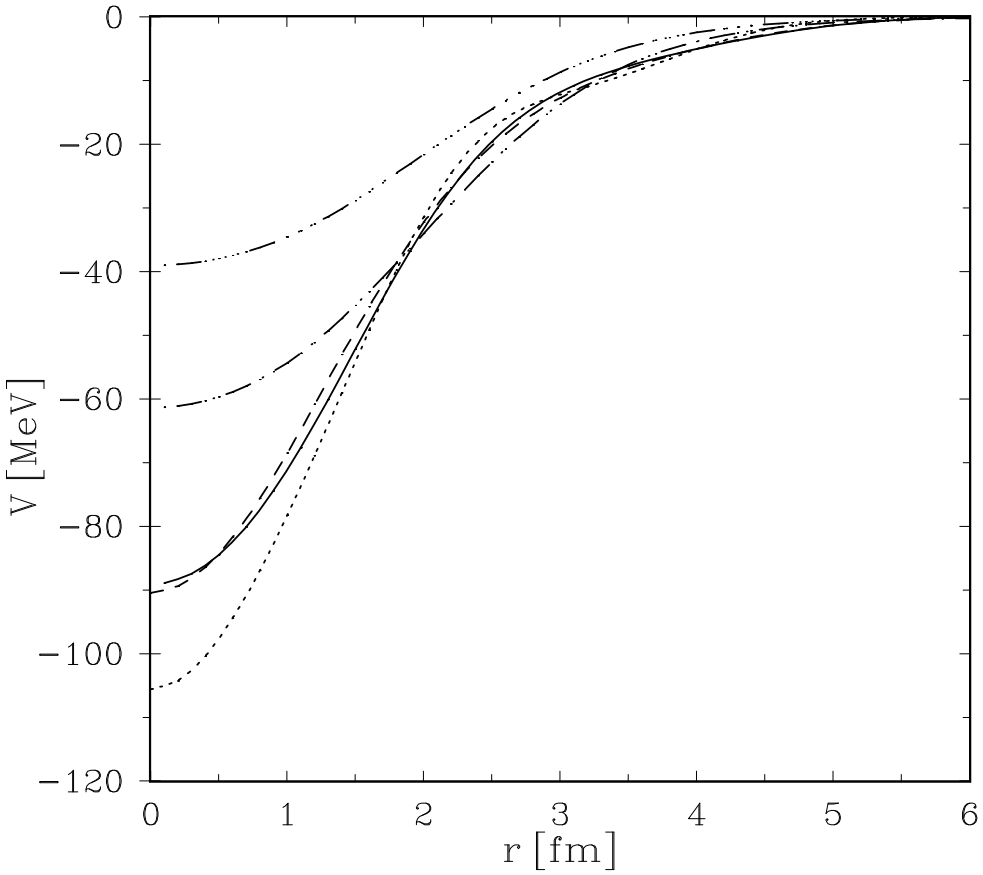
0
−20
−40
−60
−80
−100
−120
V [MeV]
0
1
2
3
4
5
6
r [fm]

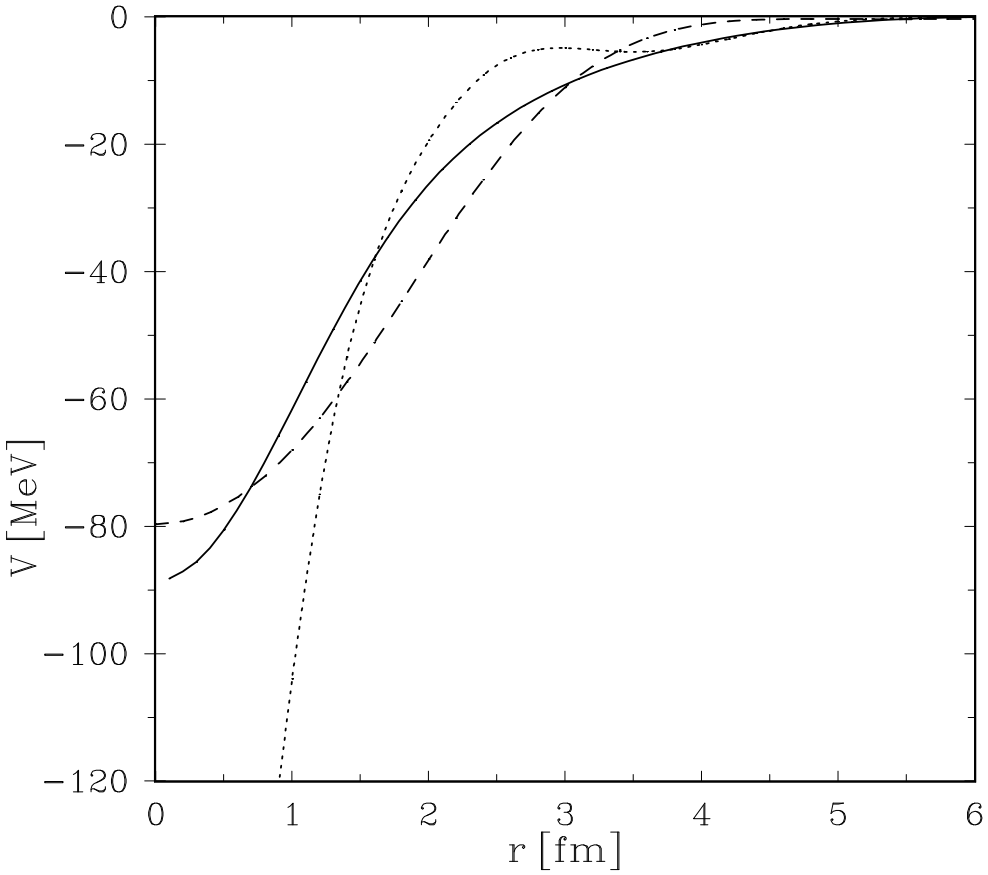
0
−20
−40
−60
−80
−100
−120
V [MeV]
0
1
2
3
4
5
6
r [fm]

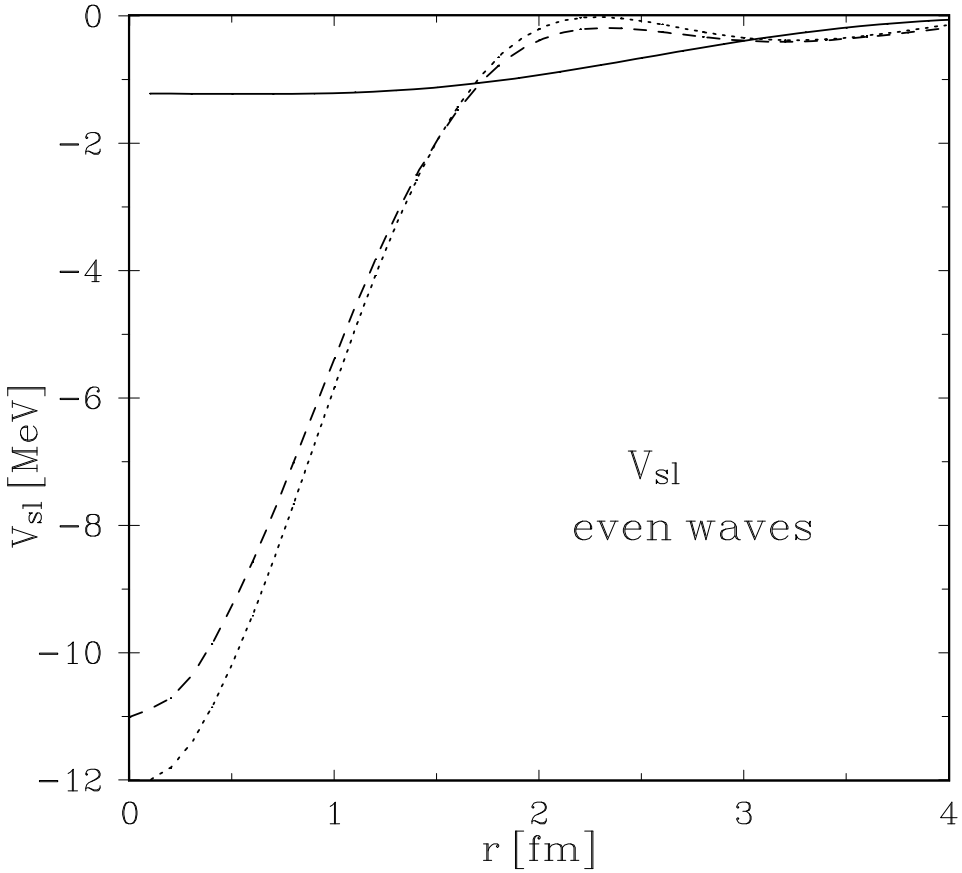
0
−2
−4
−6
−8
−10
−12
V_{sl} [MeV]
0
1
2
3
4
r [fm]
V_{sl}
even waves

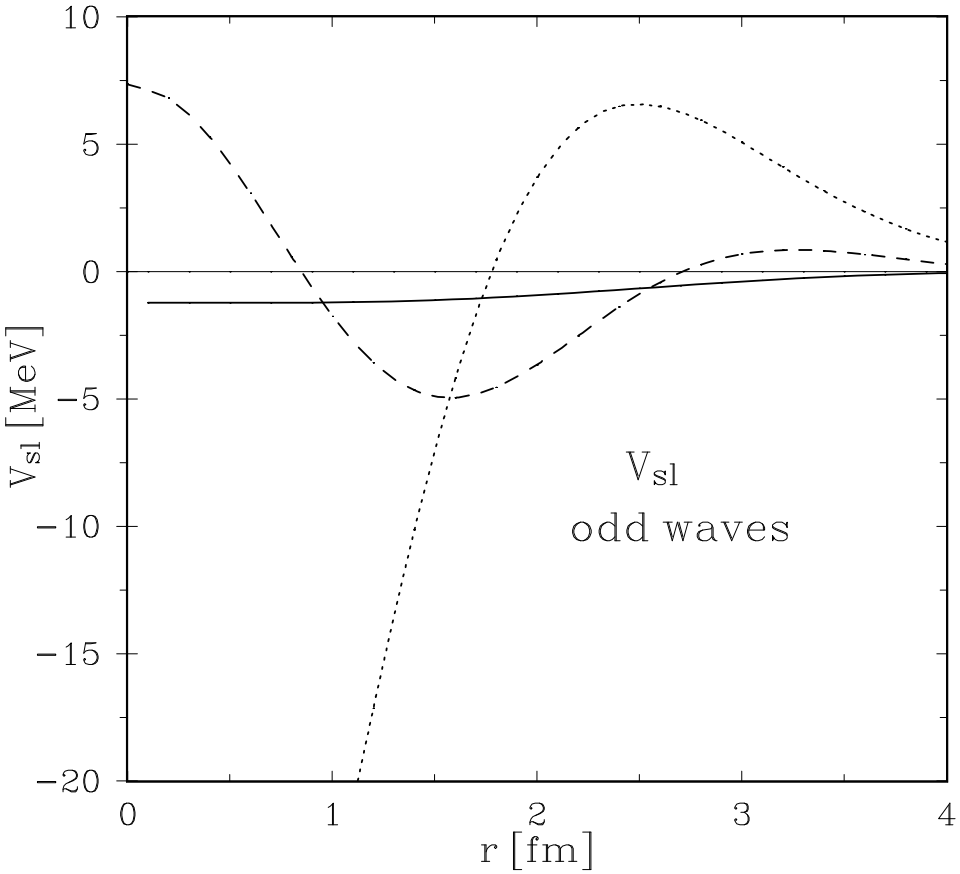
10
5
0
−5
−10
−15
−20
0
1
2
3
4
V_{sl} [MeV]
r [fm]
V_{sl}
odd waves

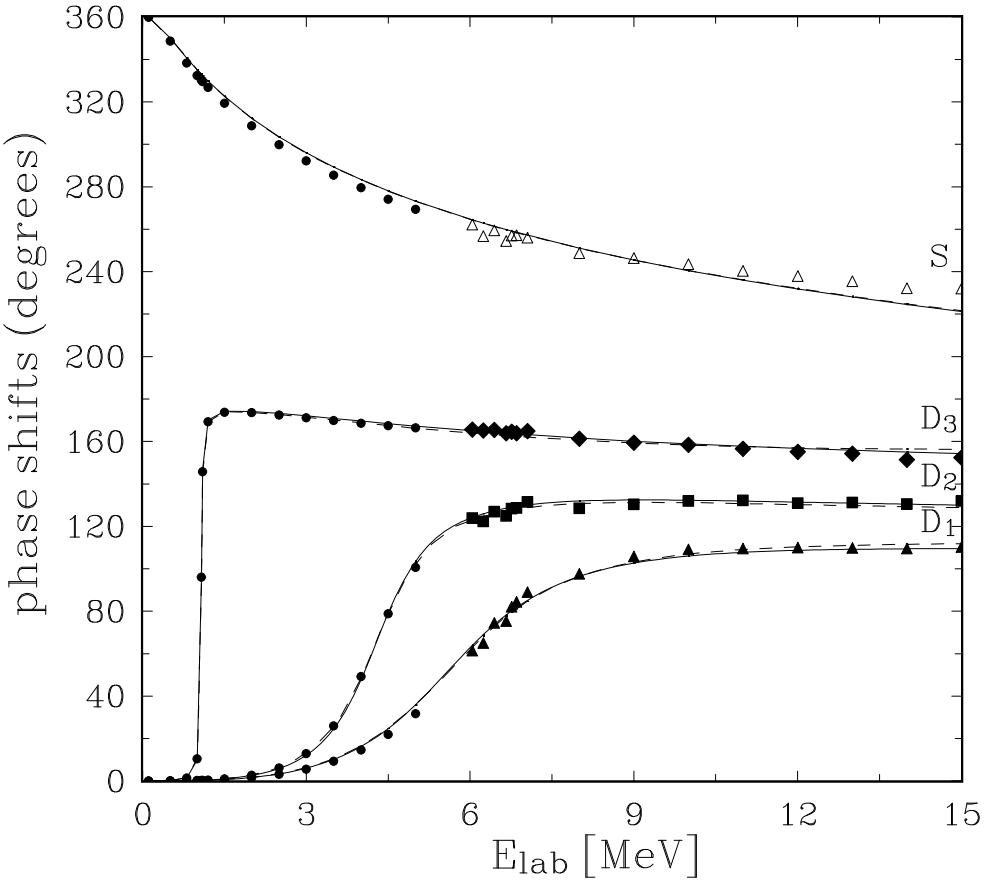
360
320
280
240
200
160
120
80
40
0
phase shifts (degrees)
0
3
6
9
12
15
E_lab [MeV]
S
D3
D2
D1

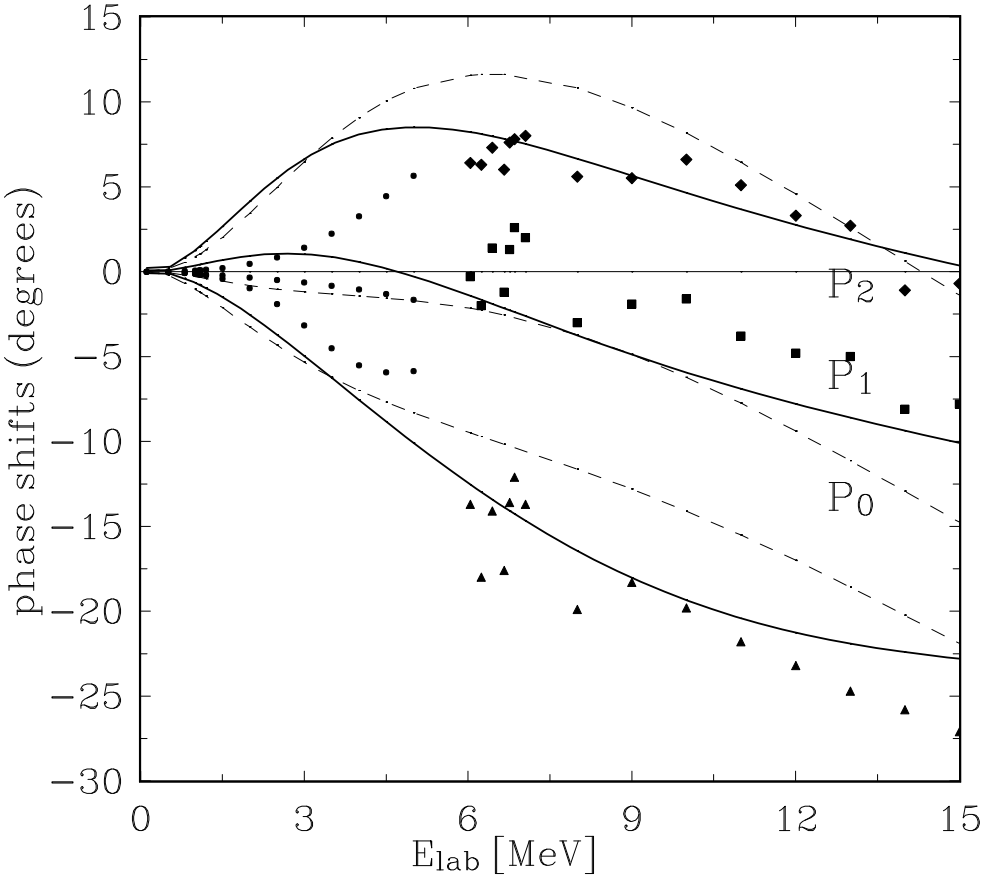
15
10
5
0
−5
−10
−15
−20
−25
−30
0
3
6
9
12
15
phase shifts (degrees)
E_lab [MeV]
P2
P1
P0

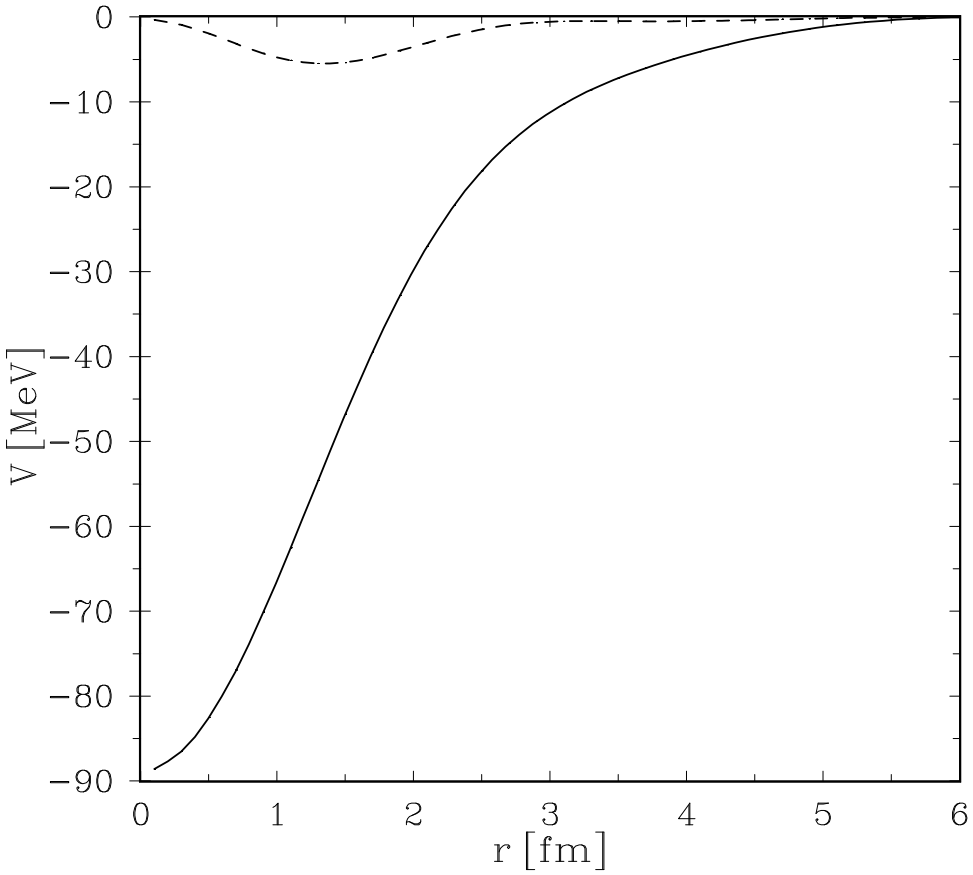
0
−10
−20
−30
−40
−50
−60
−70
−80
−90
V [MeV]
0
1
2
3
4
5
6
r [fm]

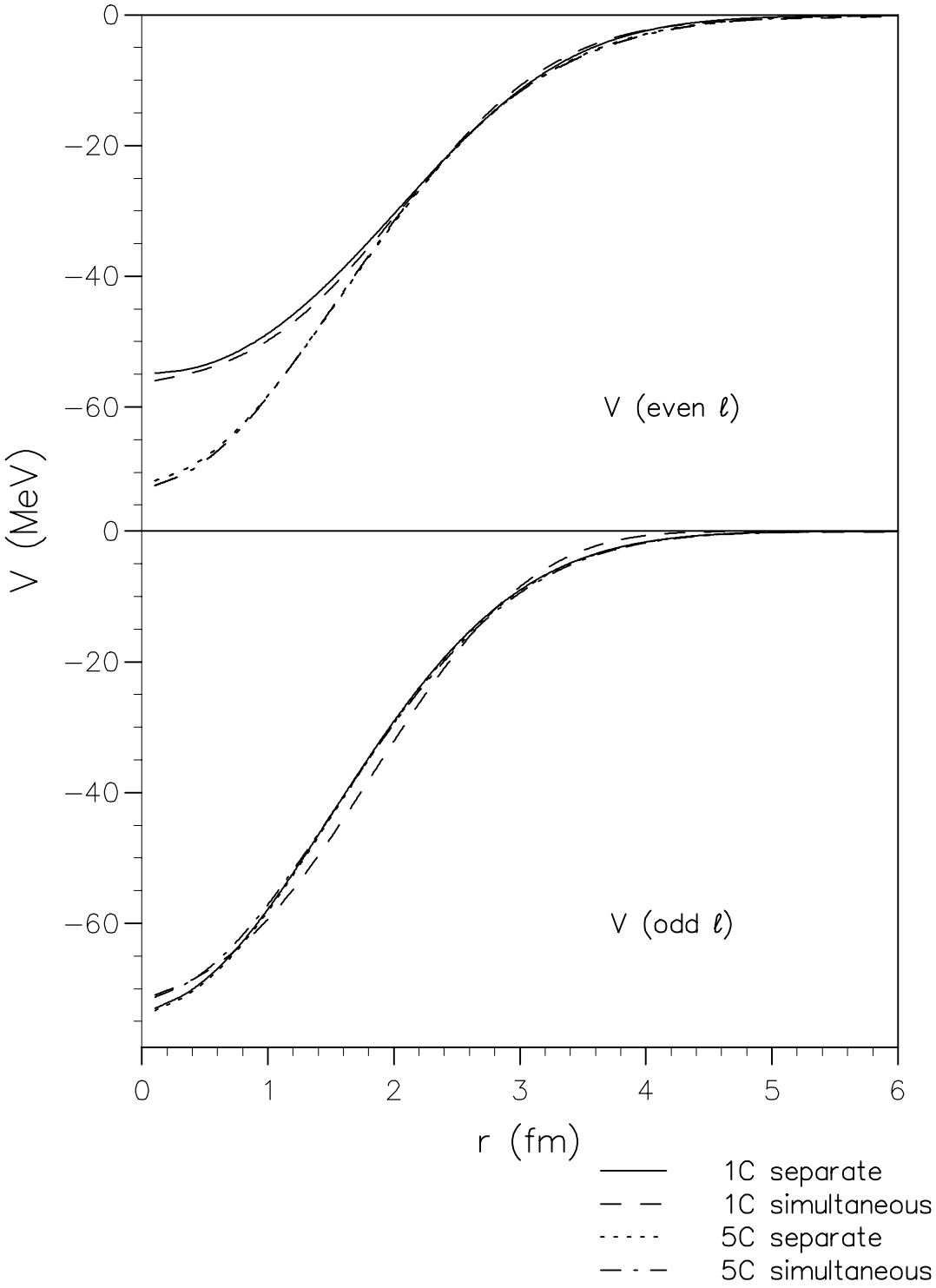
0
−20
−40
−60
0
−20
−40
−60
V (MeV)
V (even ℓ)
V (odd ℓ)
0
1
2
3
4
5
6
r (fm)
1C separate
1C simultaneous
5C separate
5C simultaneous

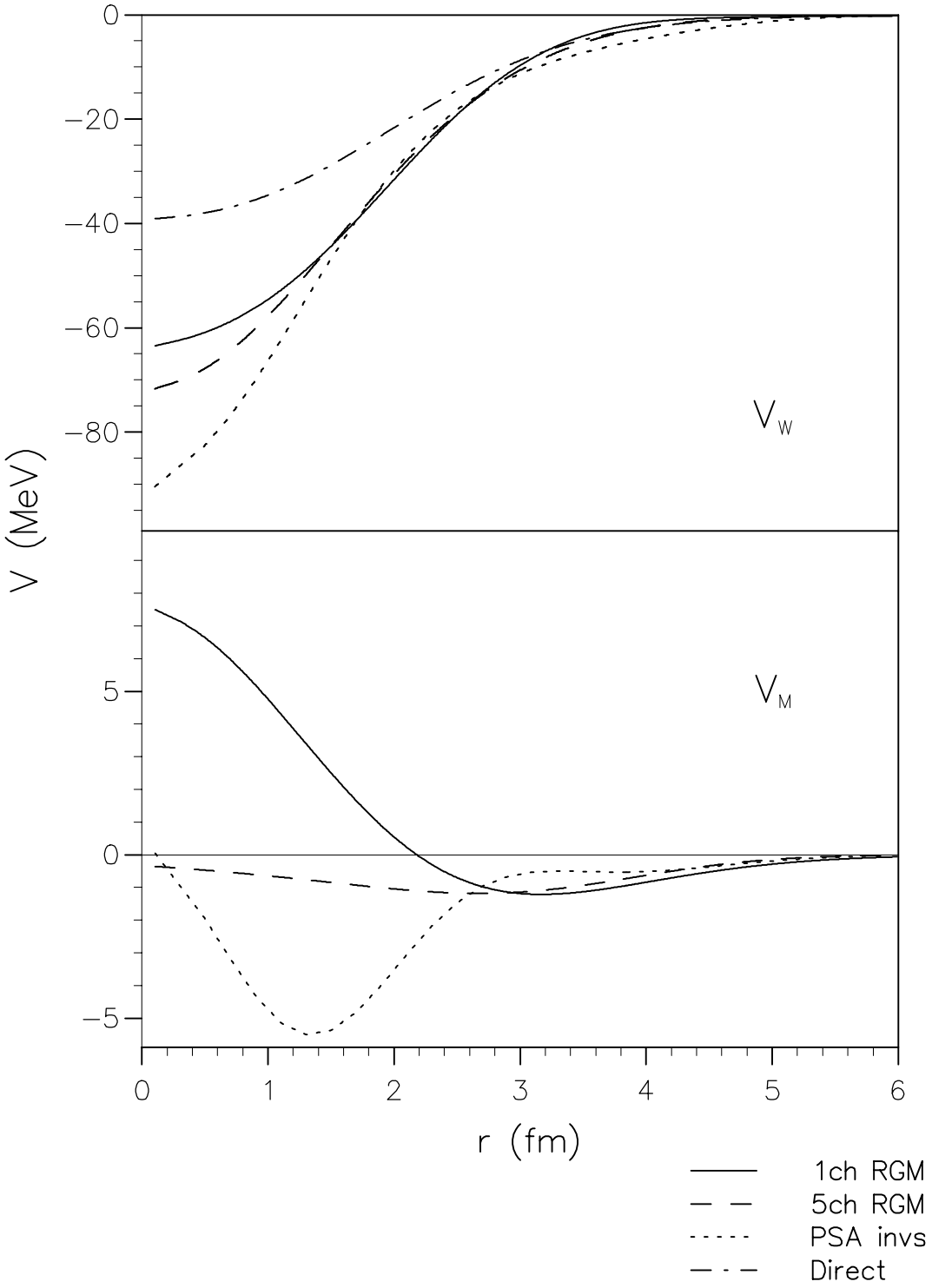
0
−20
−40
−60
−80
V (MeV)
V_W
5
0
−5
V_M
0
1
2
3
4
5
6
r (fm)
1ch RGM
5ch RGM
PSA invs
Direct

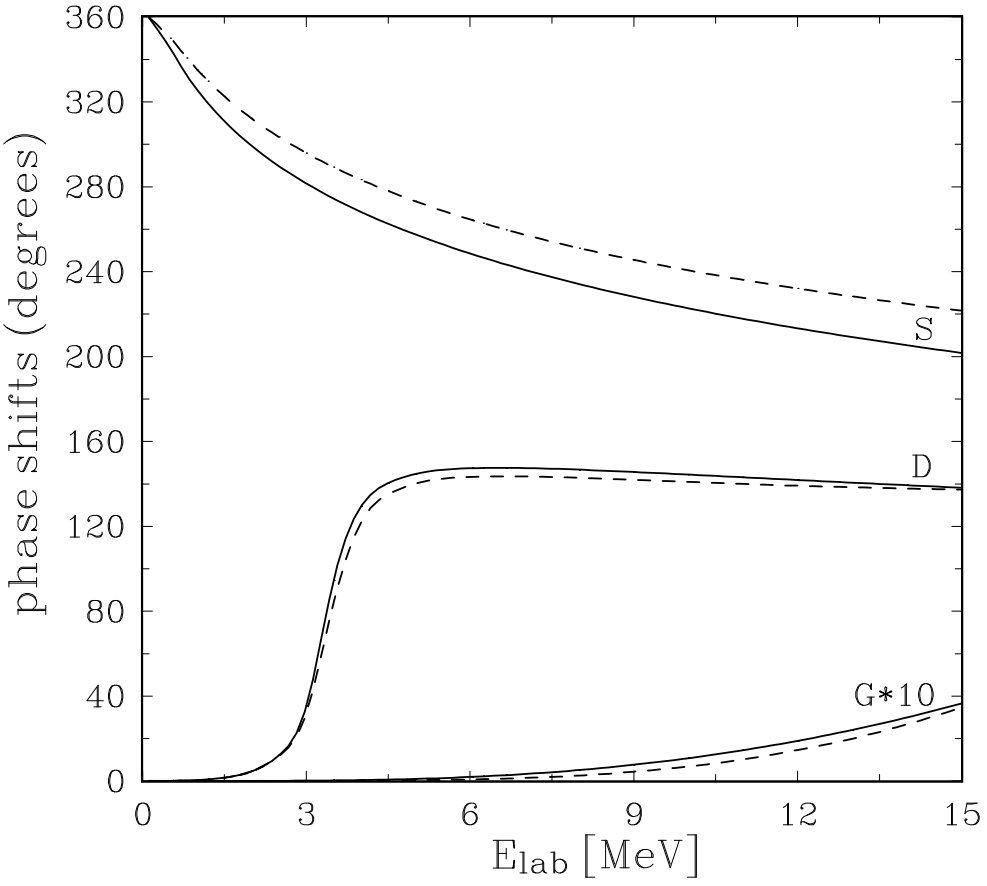
360
320
280
240
200
160
120
80
40
0
phase shifts (degrees)
S
D
G*10
0
3
6
9
12
15
E_lab [MeV]

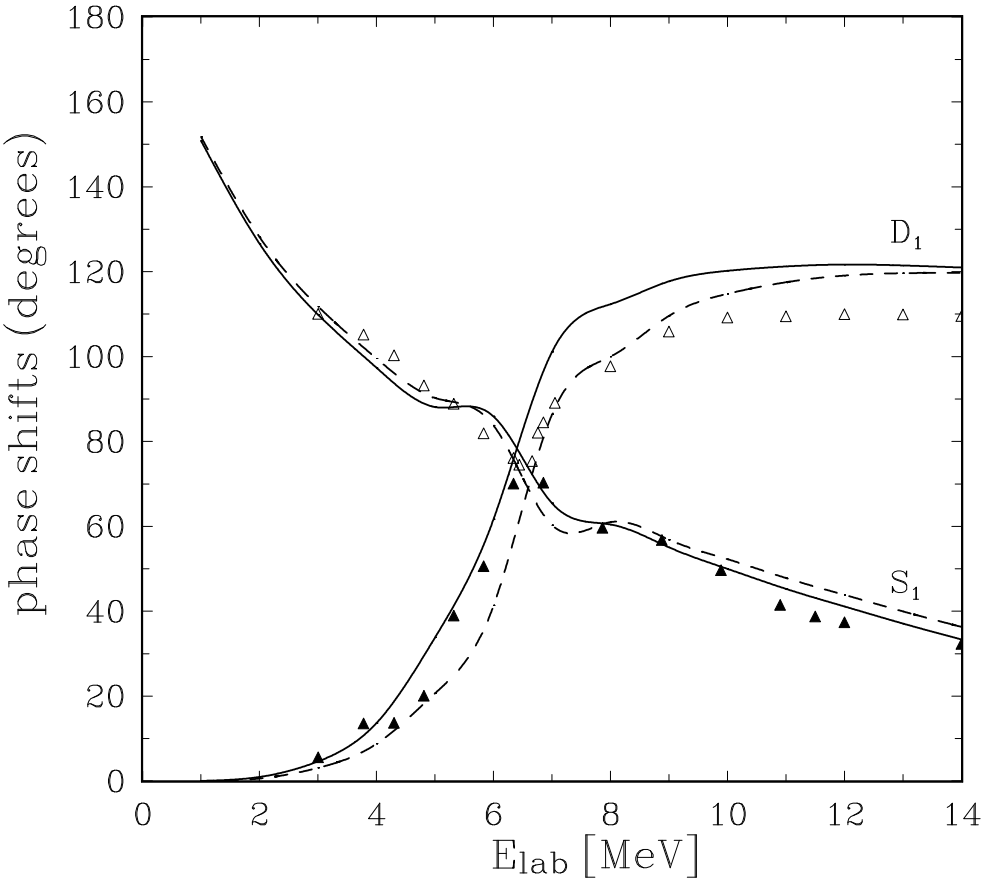
180
160
140
120
100
80
60
40
20
0
0
2
4
6
8
10
12
14
phase shifts (degrees)
E_lab [MeV]
D_1
S_1

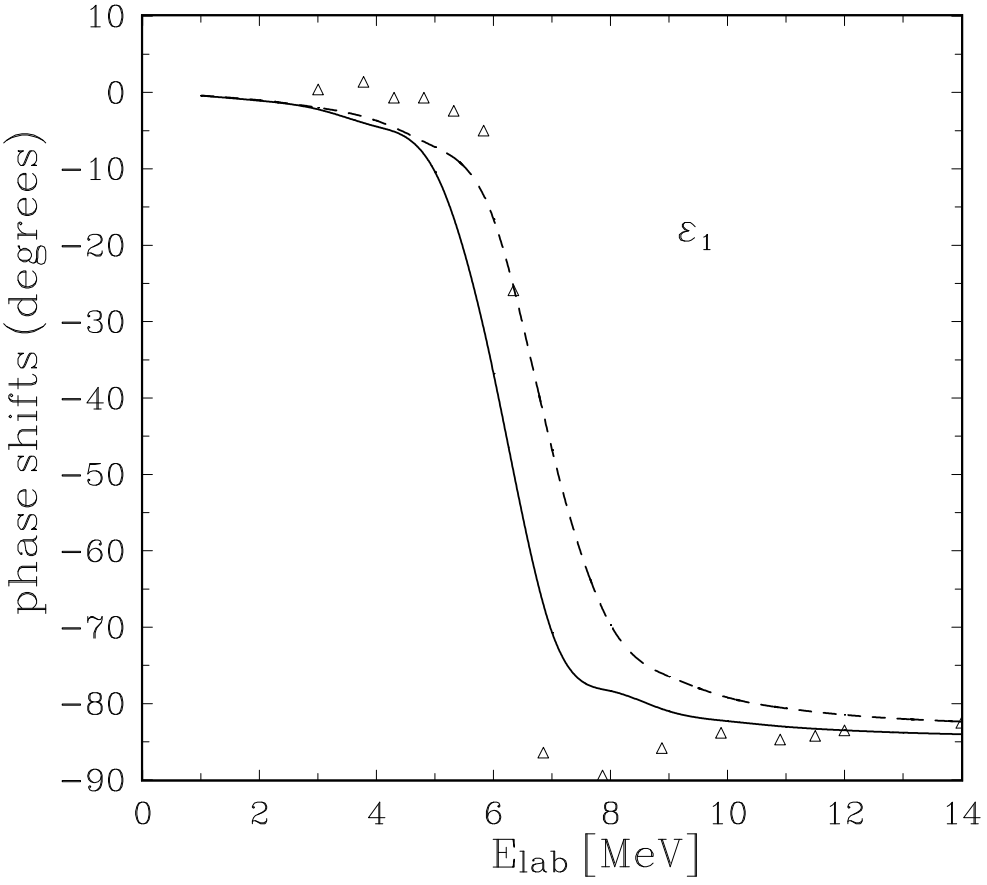
10
0
−10
−20
−30
−40
−50
−60
−70
−80
−90
0
2
4
6
8
10
12
14
phase shifts (degrees)
E_lab [MeV]
ε_1